MICROWAVE TOMOGRAPHY - CLINICAL APPLICATION

M.S.Hawley *, A.Broquetas* , L.Jofre *, E. de los Reyes *, H.Almirall**

Abstract

The clinical applications of a microwave tomographic system are studied. Imaging parameters are appropriate for medical use : a spatial resolution of 7mm and a contrast resolution of 1% for a measurement time of 3 seconds. Measurements on tissue-simulating phantoms and volunteers, together with numerical simulations are presented to assess the system for absolute imaging of tissue distribution and for differential imaging of physiological, pathological and induced changes in tissues.

Introduction

Forming images of the human body using ionising radiation has been a part of the diagnostic process in medicine for many years. More recently, other probing radiations, notably ultrasound, have provided successful diagnostic images. Tomography is now in widespread use in the clinic with ionising radiations (X-ray, isotopes) and with Nuclear Magnetic Resonance imaging. In the past few years, other probing radiations have been considered for tomography, including ultrasound [1,2], very low frequency electromagnetic fields in electrical impedance tomography [3] and microwaves [4,5].

Microwave diffraction tomography is an imaging technique which gives information on the dielectric properties of the body, data which is distinct from but complementary to other methods based on different radiations.

Research into cylindrical microwave tomography for medical applications began in Barcelona in 1985, the development of a first prototype [6], has now reached the stage where clinical application can be considered. Imaging parameters are appropriate for clinical use:- a spatial resolution of 7 mm within a useful diameter of 20 cm, a total measurement time of 3 seconds and a contrast resolution of around 1% for a change in central permittivity.

Two areas of application are being investigated. Firstly, the large variation of dielectric parameters between different body tissues allows the formation of high contrast absolute images. Secondly, dielectric parameters vary with some physiological changes and therefore differential mapping of these alterations is possible.

2. Absolute imaging

Absolute imaging implies taking single frame data sets to reconstruct images which contain information on the tissue structure of the object.

---

* Dep. de Teoría de Señal y Comunicaciones, ETS Ing. de Telecomunicación, Univ. Politécnica de Cataluña.

** Dep. de Psiquiatría y Psicobiología Clínica, Fac. de Psicología, Univ. de Barcelona.

Fig.1 shows an absolute image of a human forearm. The imaginary part of the complex permittivity image clearly shows the radius and ulna, the superficial fat layer and some less clearly-defined internal features. The values of permittivity are incorrectly reconstructed due to the fact that the object falls outside the region of validity of the first order imaging algorithm [7].

Fig.2 shows the reconstruction of the measured scattered field from a tissue-simulating phantom of a child's head. The algorithm reconstructs correctly the outer contour of the model but large oscillations exist within the model. These oscillations are due to the important perturbation produced by the object on the incident field. Such problems with the algorithm effectively limit, at the moment, absolute imaging to the limbs. A large research effort is being carried out worldwide to improve reconstruction of microwave diffraction data, and it is hoped in the future to use this technique for absolute imaging of the brain, since the substantial difference in permittivity values between different soft tissues should allow them to be be easily distinguished.

3. Differential imaging

a. Thermal change imaging

To estimate the temperature sensitivity of the system, a rubber tube 0.05mm thick and 3cm internal diameter was placed off-centre in the water tank. Water from an external temperature tank was pumped through the tube, whilst the surrounding medium was maintained at 24°C. Fig.3 shows a differential image corresponding to a temperature change of 2°C, the graph showing the linear relationship between the image values and temperature. The temperature resolution was experimentally found to be 0.5°C. It is expected that in a more lossy and diffracting medium such as the human body, the temperature resolution would deteriorate. However, this measured resolution is comparable with phantom results reported for other imaging techniques being considered for non-invasive temperature monitoring in hyperthermia.

b. Blood content imaging

In order to demonstrate the capability of imaging blood content variations, the blood content of the arm of a volunteer was varied. After holding the arm in the air to remove as much blood as possible, a pressure cuff was applied to the upper arm and pressurised to above the systolic pressure. The arm was then placed in the tank and after taking three images, the cuff was released to just above the diastolic pressure thus increasing the blood content of the arm with time. Images were taken at the rate of one every three seconds for the next 90 seconds. After 70 seconds, the cuff pressure was released completely, allowing the blood content to begin to return to normal. The series of images (Fig.4) shows a linear increase in the maximum image value until the cuff is released completely, when the image values began to fall. The images show a gradual development and change of position of the maxima.

c. Differential imaging of the head

Fig.5 shows a measured differential image of the head model, changing the inner section of the brain from a white matter equivalent liquid to water. The reconstruction shows up well the extension and form of the change. In Fig.6, a small haemorrhage in the right posterior section of the white matter is created by adding a small gel block with the dielectric properties of

blood. The image represents well the position of the haemorrhage.

4. Discussion and conclusions

The results presented show the capability of the prototype system for absolute imaging of smaller biological bodies (eg limbs) with differential imaging of induced temperature changes and blood flow changes. Measurements on a head phantom have demonstrated the system's ability to visualise alterations within the brain.

Possible clinical applications are being sought by the authors. Suggested applications include the visualisation of blood content changes in the limbs with applications in detecting thromboses, since regions with poor blood supply would show smaller changes in permittivity. A cardiac gating system is presently being added to the imaging system and should improve the imaging of blood-flow. Results show that imaging changes within the brain should be possible with the present algorithms. One possible application would be to detect brain haemorrhaging in neo-nates, although this application is expected to bring many additional practical problems. Visualisation of regional blood-flow variations within the brain due to increased specific brain activity appears feasible but will require an increase in system sensitivity. Absolute imaging of the brain will require improvement of the reconstruction algorithms.

The present system of employing a water tank is convenient for the imaging of limbs, but evidently cannot be used when the head is to be imaged. A possible solution consists of employing a bolus or water-filled bag which fits between the antennas and the head. This system was successfully employed in the early X-ray head scanners to avoid the large jump in density between the tissue and the surrounding air. As in these X-ray scanners, the bag would also serve to hold the head stationary during the scan. In a future design, the matching medium could be dispensed with altogether if contacting (possibly microstrip) antenna were placed directly in contact with the tissue.

In conclusion, a microwave scanner for rapid tomographic imaging of the body has been produced. The system has no mechanical movement and patient microwave radiation levels are below the safety standards for long exposure. The technology used is readily available and relatively inexpensive. Research will continue to improve reconstruction algorithms, increase system sensitivity and to assess the system for clinical applications.

Acknowledgements

This work has been supported by CAICYT (Spanish Committee for Sientific and Technical Research, grant no. 1165-84), FISS (Spanish National Institute fo Health, grant no. 84/2112), Spanish-French Cooperation Programme (grant no. 30/135) and Spanish-British Cooperation Programme (grant no. 17/173). Mark Hawley holds a fellowship from The Royal Society, UK.

References

[1] R.K. Mueller, M. Kaveh, G. Wade, "Reconstructive Tomography and Applications to Ultrasonics", Proc. IEEE, Vol. 67, pp. 567-587, April 1979.

[2] B. Duchene, W. Tabbara "Tomographie Ultrasonore par Diffraction", Rev. Phys. Appl. no.6, pp 299-304, June 1985.

[3] D.C. Barber, B.H. Brown, I.L. Freeston, "Imaging Spatial Distributions of Resistivity using Applied Potential Tomography," Electronics Letters, vol. 19, no. 22, pp 933-4, 1983.

[4] J.Ch. Bolomey, L. Jofre, Ch. Pichot, G. Peronnet, "Microwave Diffraction Tomography for Biomedical Applications", IEEE Trans. MTT-30, no. 11, pp 1988-2000, 1982.

[5] H. Ermert, M. Dohlus, "Microwave-Diffraction-Tomography of Cylindrical Objects Using 3-Dimensional Wave Fields", ntzArchiv, Bd. 8, H. 5, pp 111-117, 1986.

[6] L. Jofre, E. de los Reyes, M. Ferrando, A. Elias, J. Romeu, M. Baquero, J.M. Rius, "A Cylindrical System for Quasi-real-time Microwave Tomography", 16th European Microwave Conference, Dublin, September 1986, pp 599-604

[7] J.M. Rius, M. Ferrando, L. Jofre, E. de los Reyes, A. Elias, A.Broquetas, "Microwave Tomography: An Algorithm for Cylindrical Geometries", Electronics Letters, vol. 23, no. 11, pp 564-565, May 1987.

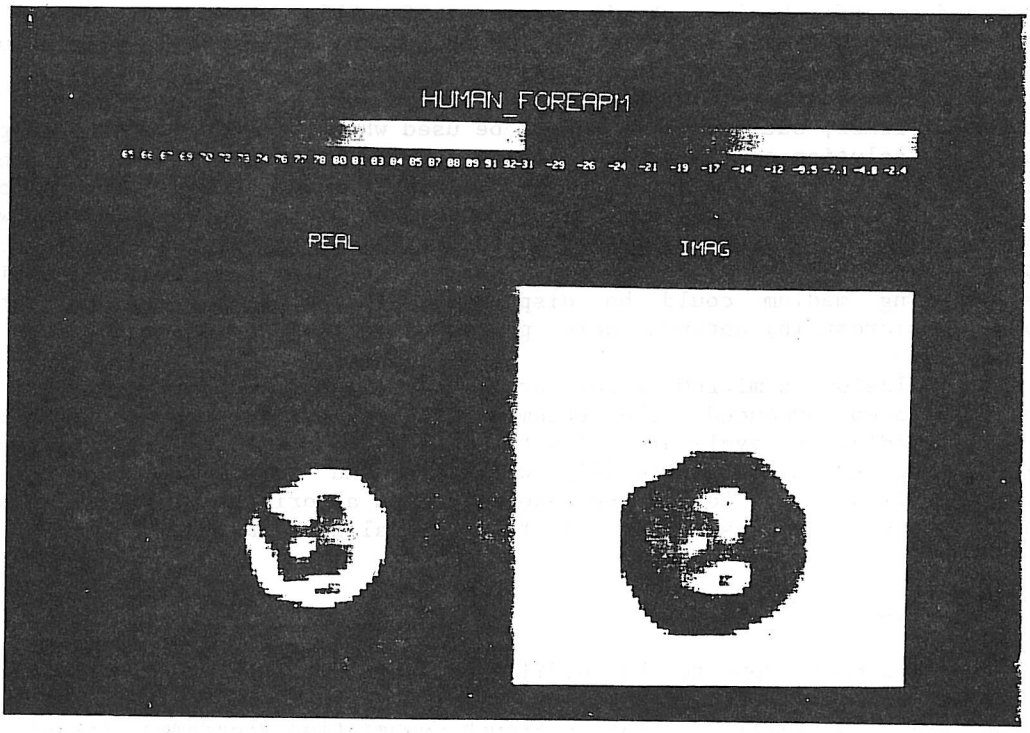

1. Tomographic slice of a human forearm.
Absolute image of complex permittivity.

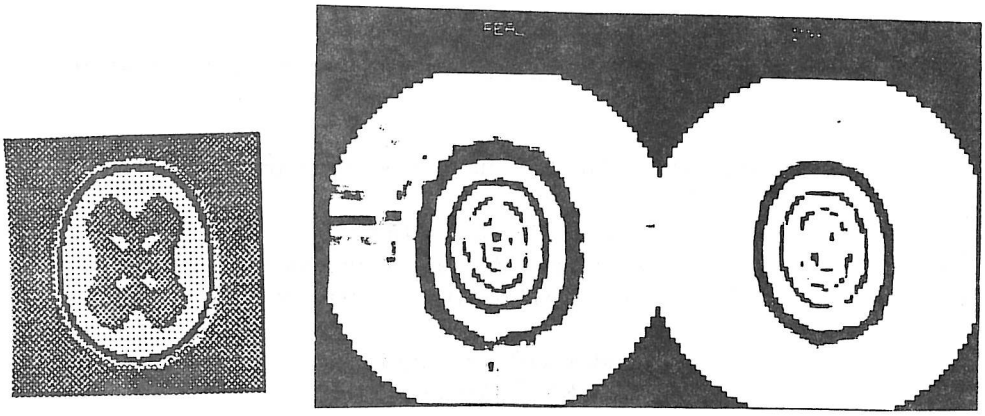

2. Phantom and its complex permittivity absolute image.

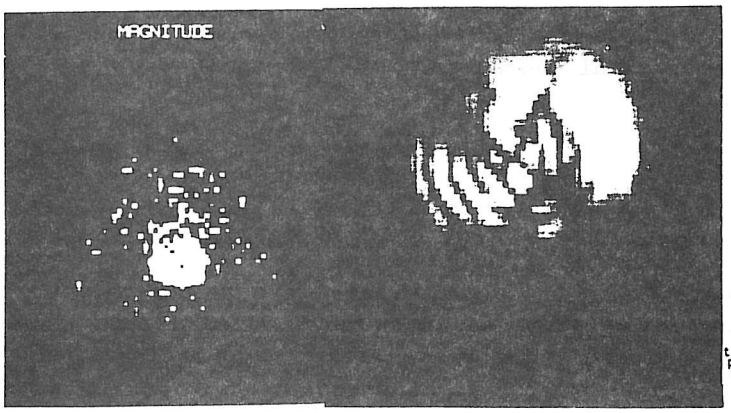

3. Image of 2°C temperature change.

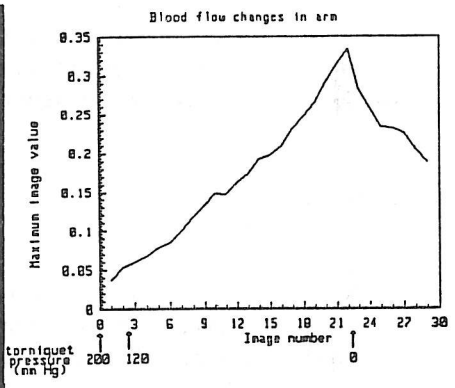

4. An image selected from a series of images of blood content change in the arm. The graph shows the maximum image value versus image No.

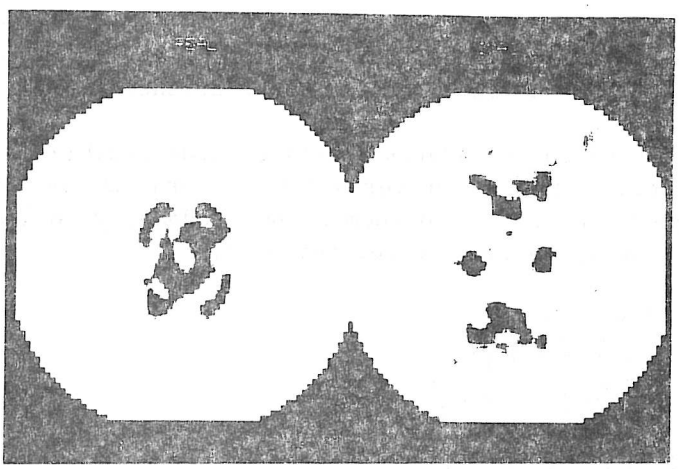

5. Head differential permittivity image obtained by substituting water for white matter equivalent liquid.

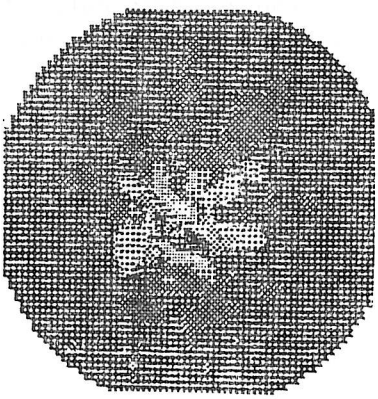

6. Differential image of an hemorrage simulation.